land

MDPI

Article

Supply–Demand Matching Assessment of Cooling Services from Urban Green Spaces in a Tropical City with Remote Sensing

Ya Huang [1], Yunxia Du [1,2,*], Zhibin Ren [3] and Yingying Zhang [1]

[1] School of Geography and Environmental Sciences, Hainan Normal University, Haikou 571127, China
[2] Key Laboratory of Tropical Island Land Surface Processes and Environmental Changes of Hainan Province, Haikou 571127, China
[3] Northeast Institute of Geography and Agroecology, Chinese Academy of Sciences, Changchun 130102, China
* Correspondence: 920219@hainnu.edu.cn

Abstract

With increasingly deteriorating urban thermal environments, urban residents have a growing demand for the cooling services of urban green spaces (UGSs). However, the spatial pattern of the supply and demand of cooling services was still not well understood, especially in tropical cities. Based on our constructed Cooling Services Supply Index (CSI) and Cooling Services Demand Index (CDI), we quantitatively assessed the supply–demand matching in Haikou, a typical tropical city. The results showed that: (1) only 54.73% of UGS patches had a measurable cooling effect in this typical tropical city. The UGS cooling distance (CD) ranged from 17.80 to 545.20 m (mean: 231.98 m), and the cooling intensity (CI) ranged from 0.06 to 9.11 °C (mean: 1.92 °C). (2) High-supply cooling-service areas were mainly distributed near large parks, urban peripheries, and industrial zones, while high-demand areas were concentrated in densely built-up central urban areas. Subdistricts in the old urban area showed high demand and low supply, whereas those in new urban areas or suburbs showed moderate surplus and low demand. (3) At the block scale, deficit, mid-deficit, and zero-supply, covering 79.63% of the population, and 91.56% of blocks and 86.81% of the population, remained below good or excellent coordination. At the subdistrict scale, five subdistricts achieved a balanced supply–demand relationship, and five reached a relatively high coordination level. (4) In central Haikou, 50.64% of the 1102 blocks were anomalous. Priority areas covered 36.31% of the population, and zero-supply, deficit-disorder, and deficit-near-disorder accounted for 97.51% of the priority-area population, indicating that critical cooling conflicts occur in densely populated areas. This study can provide strategic support for green space planning and management, as well as thermal environment governance in tropical cities.

Keywords: urban green spaces; cooling services; supply–demand evaluation; tropical city

Academic Editor: Zhonghua Gou

Received: 13 October 2026
Revised: 19 November 2026
Accepted: 20 November 2026
Published: 24 November 2026

Copyright: © 2026 by the authors. Licensee MDPI, Basel, Switzerland. This article is an open access article distributed under the terms and conditions of the Creative Commons Attribution (CC BY) license.

1. Introduction

With the acceleration of global urbanization and climate warming, the trend of urban warming has further intensified [1]. Meanwhile, a large amount of anthropogenic heat and greenhouse gas emissions in cities further exacerbate the urban heat island

(UHI), leading to frequent extreme heatwave events [2]. Extreme heatwaves can induce heat-related diseases such as respiratory and circulatory system disorders, severely harming human health and even causing fatalities [3]. Urban green spaces (UGSs) are recognized for their significant ecological and environmental benefits, including cooling, humidifying, carbon sequestration and oxygen release, noise reduction, pollution mitigation, and biodiversity maintenance [4,5]. Among these, the cooling effect of green spaces is considered an effective means of mitigating UHI. UGSs reduce solar radiation through vegetation shading, absorb ambient heat via transpiration, take in carbon dioxide through photosynthesis, and lower urban land surface temperature (LST) [6]. Therefore, how to enhance the cooling services efficiency of UGSs and mitigate the UHI has become a critical issue for maintaining sustainable urban development [7].

Numerous studies have shown that UGSs have a significant mitigating effect on the UHI, and their cooling effect has been widely confirmed. Currently, researchers often explore the relationship between different landscape elements and the cooling effect of green spaces from the perspectives of landscape composition and spatial configuration, thereby revealing how the composition and evolution of green spaces' landscape patterns affect UHI [8]. At present, studies on the cooling effect of green spaces often use indicators such as cooling distance (CD), cooling area (CA), cooling intensity (CI), and cooling gradient to evaluate the cooling effect of UGSs [9]. Research has shown that the cooling benefit of UGSs is influenced by multiple factors and varies across different urban environments [10]. There were significant differences in the cooling effect of UGSs among different cities: cities in subtropical monsoon climate zones and northeastern China showed higher CI, while northern cities had larger CD [11].

Currently, most existing studies focus on large and medium-sized inland cities in temperate and subtropical regions [12]. Although the thermal environment of coastal cities may be moderated by marine influences [13], tropical coastal cities still experience hot and humid weather and severe urban thermal environmental pressure, creating an urgent need for cooling services. However, only a few studies have focused on coastal cities, and research on the mitigation of UHI by UGSs in tropical coastal cities remains insufficient [14]. Meanwhile, existing studies on the supply–demand balance of UGSs have mostly focused on park green spaces (PUGSs), with less attention paid to the spatial differences in the cooling services supply of UGSs [15]. Due to significant spatial disparities in the distribution of UGS resources and the limited cooling services range they provide, a mismatch arises between cooling resources and cooling demand [16]. Urban built-up areas are widely distributed, with intensive socioeconomic activities and large populations, while the amount of UGSs is relatively insufficient, resulting in high cooling demand but limited supply capacity [17].

Regarding supply–demand assessment, some scholars have evaluated the equity of PUGSs supply and demand [18,19]. Existing research consistently demonstrates that significant supply–demand mismatches and spatial disparities characterize both the spatial allocation of UGSs and the supply–demand evaluations of diverse ecosystem services delivered by UGSs [20–22]. Meanwhile, some studies have assessed the supply–demand relationship of blue–green spaces' cooling. Most studies indicate that there is a supply–demand mismatch in the mitigating effect of urban blue–green spaces on the UHI [23,24] . Nevertheless, despite being a critical ecological function of UGSs, the supply–demand relationship of UGS cooling services remains understudied in a systematic manner.

Regarding quantitative assessment methods for supply–demand matching relationships, some existing studies adopt a single supply–demand ratio or the four-quadrant method to evaluate multiple functions of UGS ecosystems [25,26]. These approaches can only characterize the quantitative matching relationship between supply and demand.

In contrast, the coupling coordination degree (CCD) model can dynamically assess the interaction and coordination between the two dimensions of supply and demand from a systematic perspective, with a stronger focus on their qualitative relationship [27]. To date, this model has been widely applied in various research fields, including ecosystem services, socioeconomic conditions, and urban resilience [28–30].

Overall, although numerous studies have confirmed that UGSs can provide cooling services [31], research focusing on tropical regions remains relatively limited [32]. Meanwhile, urban areas contain a large number of non-park urban green spaces (NPUGSs), whose cooling effects can serve residents within a certain spatial range, yet such UGSs are frequently overlooked in current research [33]; most existing studies predominantly concentrate on the basic supply–demand relationships of PUGSs, leaving a notable research gap in the systematic assessment of supply–demand dynamics of cooling services functions [34]. To date, there is still a lack of integrative studies that examine UGS services in tropical humid regions from a supply–demand evaluation perspective.

To address the above research limitations, this study incorporates both park green spaces and non-park urban green spaces and quantifies the cooling contribution of each green patch. On this basis, it further integrates the supply–demand ratio with the coupling coordination degree (CCD) model, moving beyond conventional quantitative supply–demand matching methods that cannot reflect the interaction between the two systems. This approach can simultaneously assess the quantitative matching and the degree of interaction and coordination, thereby achieving an integrated, process-oriented assessment.

Haikou is a typical tropical coastal city characterized by high temperature and high humidity. In recent years, with continuous population growth and accelerating urban construction, the UHI has become significant, and urban residents have a strong demand for cooling. Currently, Haikou is experiencing rapid urban expansion, and the supply of UGS cooling services is insufficient to meet the growing demand. This study encompassed three key aspects: (1) exploring spatial patterns of supply and demand for UGS cooling services; (2) revealing cooling services matching and coordination characteristics; (3) identifying the spatial distribution of composite classification based on supply–demand status and coupling coordination degree, as well as priority intervention areas. Our study can provide policy and strategic support for UGS planning and management, as well as for the equalization of public services.

2. Materials and Methods

2.1. Study Area

Haikou is located in the northern part of Hainan Island (19°31′32″–20°04′52″ N, 110°07′22″–110°42′32″ E) with a land area of 2296.82 km^2, facing Xuwen County of Guangdong Province across the sea to the north (Figure 1). Haikou is a typical humid tropical coastal city, situated in a low-latitude tropical region with a tropical monsoon climate. The city experiences high temperatures throughout the year without severe cold weather, and the annual average temperature is 25.2 °C. The terrain is low in the middle and high in the northwest and southeast, with gentle relief. The permanent resident population of Haikou is 3.0016 million in 2023, of which the urban population accounts for 72.73%. The gross domestic product (GDP) of the city is 235.844 billion yuan. The total area of UGSs is 8961.98 ha, and the per capita public green spaces area is 12.08 m^2. This study selected the central urban area of Haikou as the study area, bounded by Changtian Road to the west, the Nandu River to the east, the coastline to the north, and the urban built-up area between Yehai Avenue and the Ring Expressway to the south. The area includes 21 subdistricts of Haikou, as well as parts of Chengxi Town and

Haixiu Town. This region is one of the earliest developed areas of Haikou, with a long history of development and a high concentration of population. The dominant land use types are residential land and industrial land. The block data for this study were generated based on road network data from OpenStreetMap (OSM, https://www.openstreetmap.org). A complete block polygon layer was constructed through steps including road clipping, centerline extraction, and topological optimization.

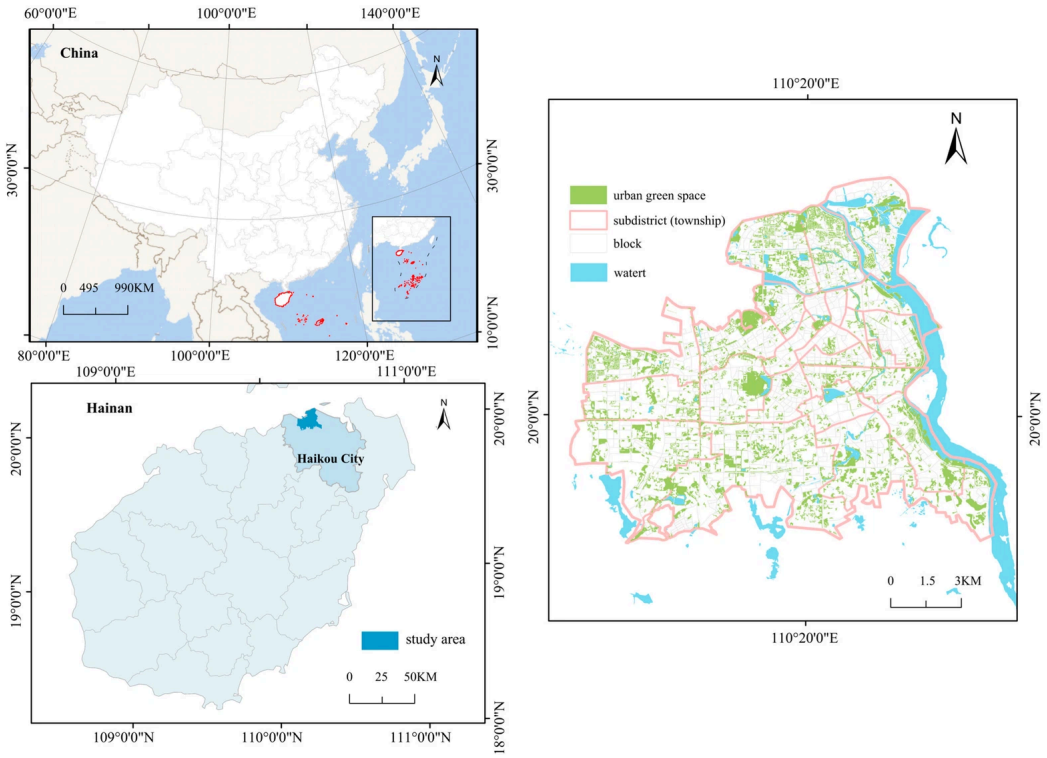


Figure 1. Study area and distribution of UGSs. The red area indicates Hainan Province, China, while the study area is the main urban area of Haikou City, which lies within it.

2.2. The Research Framework for Our Study

First, Landsat 8 land surface temperature (LST) data were used, and a buffer analysis combined with cubic polynomial fitting was applied to quantify the cooling distance (CD) and cooling intensity (CI) of UGSs. Based on this, a Cooling Services Supply Index (CSI) and a Cooling Services Demand Index (CDI) were constructed to characterize the spatial distribution patterns of cooling supply and demand. Second, a supply–demand ratio was used to identify structural mismatch patterns of cooling services. Third, a coupling coordination degree (CCD) model was introduced to evaluate the interaction between cooling supply and demand systems, capturing their systemic coordination characteristics. Finally, we overlaid supply–demand classification with the coupling coordination degree (CCD) to derive the composite classification based on supply–demand status and coupling coordination degree and map their spatial distribution, thereby delineating priority intervention areas and non-anomalous regions (Figure 2).

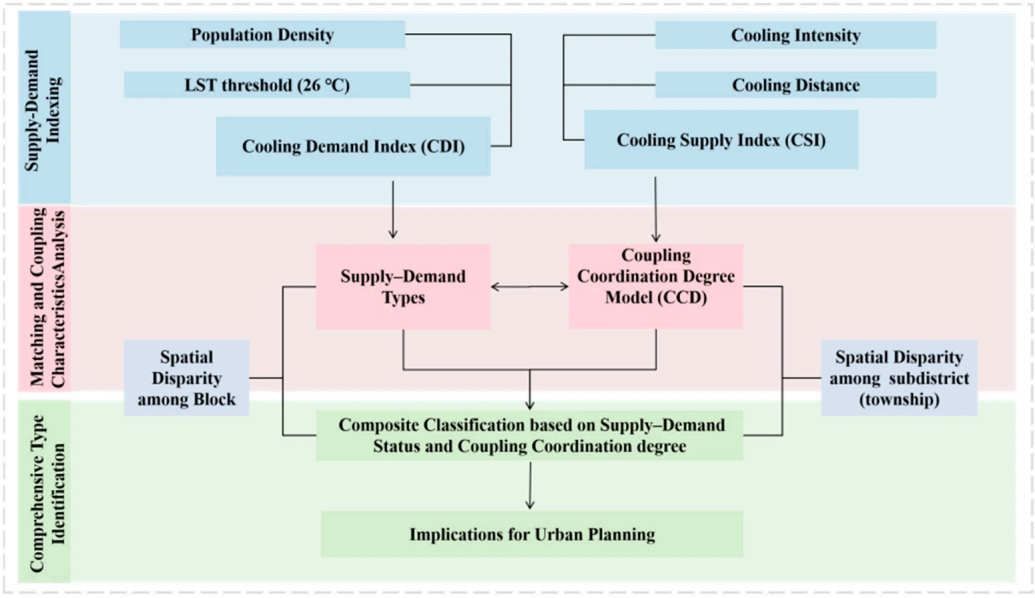


Figure 2. The workflow of this study.

2.3. Data Sources

2.3.1. Urban Green Spaces' Pattern

Urban green spaces boundaries were obtained from the UBGG-3m fine-grained urban blue–green-gray landscape dataset covering 36 Chinese cities [35]. This dataset was generated by classifying satellite imagery acquired in the summers of 2021 and 2022 and reports an overall accuracy of 91.23% for urban land cover classification, with F1-scores (the harmonic mean of precision and recall) ranging from 85.97% to 95.15% across all classes. Considering the relatively limited function of small isolated green-space patches and referring to existing studies [36], as well as the Standard for Urban Residential Area Planning and Design (GB 50180-2018)[37], independent green-space patches larger than 0.4 ha were extracted, yielding a total of 1195 green-space patches (Figure 1). On this basis, park green spaces (PUGSs) were identified using Amap park POI data (2022), together with visual interpretation: the POI records served to determine the park attribute of each patch and to discard entries that had a POI record but no corresponding vegetated entity. Patches that were not attributable to parks but still functioned as urban green spaces were retained as non-park urban green spaces (NPUGSs).

2.3.2. Land Surface Temperature (LST)

In Haikou, the wet season (May–October) is characterized by frequent cloud and fog, and only the image acquired on 17 September 2022 had lower the cloud-cover criterion (<10%). The LST from this image can represent the typical high-temperature thermal environment of the city. LST data were acquired via the Google Earth Engine (GEE) platform, sourced from the Landsat 8 OLI/TIRS Collection 2 Level-2 Surface Temperature (ST) Product. The ST_B10 band is generated by the USGS single-channel algorithm and already includes radiometric calibration and atmospheric correction, directly providing LST in Kelvin. The LST was then converted to °C using the official scale factor and offset:

$$\mathrm{LST}\,(^{\circ}\mathrm{C}) = (\mathrm{ST_B} \times 0.00341802 + 149.0) - 273.15 \quad (1)$$

2.3.3. Population Data

Population estimation was based on the China Multi-Attribute Building (CMAB) dataset, which provides building footprints and heights derived from approximately 0.3 m resolution Google Earth imagery. The version used in this study was based on imagery primarily acquired in 2021–2022, with a roof extraction accuracy of 91.59% (F1 = 89.93%) and building height estimation validated through street-level observations (R^2 = 0.72–0.80) [38]. Residential buildings were extracted, the housing floor area of each building was computed from its height and footprint area, and the population of each building was obtained using the per capita housing floor area of 32.1 m^2 (Haikou Statistical Yearbook 2023) [39]. The estimates were then corrected at the subdistrict level against the subdistrict permanent population enumerated in the Seventh National Population Census (2020). The specific formula is as follows:

$$CP_j = \frac{RA_j \times F_j}{HA} \times \lambda \quad (2)$$

where CP is the number of residents of building j; *RA* is the footprint area of building j (m^2); F_j is the number of storeys of building j, estimated as the building height divided by 3 m (i.e., $F_J = H_j/3$, assuming an average floor height of 3 m); and HA is the per-capita housing area (m^2); λ is the adjustment coefficient.

A Pearson correlation analysis was conducted at the block scale to assess the consistency between the building-based population estimates and the WorldPop gridded population dataset (https://www.worldpop.org/) The results revealed a strong and statistically significant positive correlation between the two population estimates (r = 0.80, $p < 0.001$), suggesting that their spatial distribution patterns were broadly consistent.

2.4. Data Analysis

2.4.1. Urban Green Spaces Cooling Services

Remote sensing methods were used to estimate the cooling intensity (CI) and cooling distance (CD) of urban green spaces (UGSs) in order to measure the cooling-service benefits of UGSs. Since the resolution of the LST data used in this study was Landsat 8 land surface temperature products with a spatial resolution of 30 m, a buffer analysis was conducted at 30 m intervals, dividing the area around each UGS boundary into consecutive buffer zones extending up to 600 m. This maximum buffer distance was selected based on previous studies; a 600 m buffer ensures complete capture of the cooling influence range while minimizing unnecessary computation [40,41]. Zonal statistics tools were used to calculate the mean temperature of each buffer zone, and adjacent UGS pixels were excluded during the averaging process to avoid potential interference from neighboring green spaces. Most existing studies indicate that the variation curve of LST in the environment surrounding UGS follows a cubic polynomial fitting trend. LST of each ring was therefore fitted as a function of distance from the patch edge. Fit quality was reported as the coefficient of determination R^2, and the accepted fits had a mean R^2 of 0.80.

$$T(x) = ax^3 + bx^2 + cx + d \quad (3)$$

where T(x) is the mean LST at a certain buffer distance around the UGS, and a, b, c, and d are the cubic coefficient, quadratic coefficient, linear coefficient, and constant term of the fitted curve, respectively.

The LST around a UGS increases with distance from the patch edge and begins to decrease after reaching a certain turning point. The first maximum point on the curve within the 0–600 m range (where the first derivative equals zero and the second derivative is negative) is defined as the cooling distance (CD), representing the maximum distance at which the green patch still exerts a measurable cooling effect beyond its boundary.

The CI is defined as the difference between the mean LST inside the UGS and the LST at the turning point.

$$\Delta T = T_b - T_g \tag{4}$$

where ΔT is the CI, T_b is the LST at the turning point, and T_g is the mean LST inside the UGS.

2.4.2. Supply Index (CSI) and Demand Index (CDI) of Cooling Services

In this study, a cooling supply index (CSI) and a cooling demand index (CDI) were constructed to evaluate the cooling-service provision of urban green spaces (UGSs) and the corresponding population demand. For the CSI, the cooling distance (CD) of each UGS was used as its effective service radius, within which the cooling benefit of the green patch is detectable. A spatial distance-decay model was then applied to estimate the magnitude of cooling service received at each location, where cooling intensity gradually diminishes with increasing distance from the patch edge. Since the same location may simultaneously fall within the cooling influence range of multiple UGSs, the total cooling supply at a given point is the cumulative superposition of benefits from all adjacent green patches, each weighted by its respective distance-decay function [42]. The CDI was used to measure the intensity of demand for cooling services. It combines LST and population density to reflect the urgency of residents' demand for cooling services under high-temperature conditions. According to existing studies, this study set 26 °C as the critical threshold for defining areas with cooling services demand [43,44].

$$CSI_i = \sum_{j=1}^{n} r_{ij} \times CI_j \tag{5}$$

where i is the block index, j is the index; CI_j is the CI of the j-th UGS (°C); r_{ij} is the distance decay coefficient representing the decay pattern of the cooling effect of UGS j on block i, calculated as:

$$r_{ij} = \begin{cases} 1 - \dfrac{d_{ij}}{CD_j} & \text{if } d_{ij} \le CD_j \\ 0 & \text{if } d_{ij} > CD_j \end{cases} \tag{6}$$

where d_{ij} is the straight-line distance from the block center point to the UGS (m), and CD_j is the CD of the UGS (m).

$$CDI_i = \max(0, LST_i - 26) \times PD_i \tag{7}$$

where LST_i is the mean LST of the i-th block (°C); 26 °C is the threshold, following previous LST-based heat-exposure assessments [45]; and PD_i is the population density.

2.4.3. Classification of Supply–Demand Relationship Type

To evaluate the supply–demand relationship of urban green spaces cooling services and identify areas where supply and demand were relatively balanced or imbalanced, the cooling-service index (CSI) and the cooling demand index (CDI) were normalized separately into dimensionless scores using min–max standardization:

$$S = \frac{CSI_i - CSI_{min}}{CSI_{max} - CSI_{min}}, \quad D = \frac{CDI_i - CDI_{min}}{CDI_{max} - CDI_{min}} \tag{8}$$

The classification is determined based on the supply–demand ratio as follows:

$$R_i = \frac{S}{D} \tag{9}$$

Combined with the service gap areas identified above, the supply–demand relationship types of cooling services were classified as follows. Blocks with no cooling supply (S = 0) were classified as zero supply, and blocks with positive supply but no cooling demand (D = 0) were classified as zero demand; these two groups were excluded from the ratio-based classification. Among the remaining blocks with both supply and demand greater than zero, those with $R > 2.0$ were classified as surplus and those with $1.2 < R \leq 2.0$ as mid-surplus, indicating that supply exceeds demand in these areas, that their cooling capacity is relatively abundant, and that they have the potential to accommodate future demand growth; $0.8 < R \leq 1.2$ as balance, indicating that supply and demand are basically in equilibrium; $0.5 < R \leq 0.8$ as mid-deficit; and $R \leq 0.5$ as deficit, indicating a shortage of cooling services and higher heat exposure for residents.

2.4.4. Coupling Coordination Degree (CCD) Model

The coupling coordination degree (CCD) model was employed to evaluate the coordination relationship between cooling services supply and demand by integrating indicators from both the supply and demand systems [46]. Zero-supply and zero-demand blocks are not assigned a CCD stage

$$C = \left(\frac{2 \times \sqrt{S \times D}}{S + D} \right)^{\rho} \tag{10}$$

where S is the normalized CSI (CSI norm), D is the normalized CDI (CDI norm), both ranging in [0, 1]; ρ is an adjustment coefficient used to enhance the discrimination of the coupling degree. Referring to existing studies, it is set to 2 [47,48]. The coupling degree ranges in [0, 1]. A value closer to 1 indicates a tighter interaction between supply and demand, whereas a value closer to 0 indicates that the two are independent or weakly interacting.

$$DI = \alpha \times S + \beta \times D \tag{11}$$

where DI is the comprehensive evaluation index; α and β are weight coefficients representing the importance of supply and demand in the system, respectively [49]. In this study, supply and demand are considered equally important, with $\alpha = \beta = 0.5$ The value of DI ranges in [0, 1].

The calculation of the CCD is as follows:

$$CCD = \sqrt{(C \times DI)} \quad (12)$$

where CCD is the coupling coordination degree, C is the coupling degree, and DI is the comprehensive evaluation index. This reflects the supply–demand matching relationship and the overall quality of the match; a larger value indicates better quality.

Blocks were aggregated to the subdistrict/township level within each administrative boundary. Population and area were summed, while the normalized supply and demand were aggregated as an area-weighted mean using block area as the weight. The subdistrict supply–demand ratio and CCD were then computed from these weighted values following the same procedure as at the block level.

2.4.5. Composite Classification Based on Supply–Demand Status and Coupling Coordination Degree

By overlaying the areas with supply–demand anomalies and low coordination degree, the spatial areas of service deficiency, surplus, deficit, mid-deficit, disorder, and near-disorder are superimposed. Based on the characteristics of these two dimensions, further subdivision is conducted into four types: surplus-disorder, surplus-near-disorder, deficit-disorder and deficit-near-disorder. The remaining areas are classified as non-anomalous types.

3. Results

3.1. Cooling Effect of Urban Green Spaces in Tropical City

In this study, 54.73% of UGS patches (a total of 1195 patches) had a measurable cooling effect, defined as cooling urban green spaces (CUGSs), including 13 park green space patches, while the remaining non-cooling urban green spaces (non-CUGS) were mainly distributed in coastal areas, along the Nandu River, and around large water bodies(Figure 3). The CD of UGSs ranged from 17.8 m to 545.2 m, with a mean of 231.98 m. The CI varied between 0.06 °C and 9.11 °C, with an average of 1.92 °C (Figure 4).

At the subdistrict (township) scale, substantial spatial heterogeneity was observed. Lantian Subdistrict exhibited the greatest average CD of 350.06 m, while Jinyu Subdistrict showed the highest average CI of 2.45 °C (Table 1). As shown in Table 2, Chengxi Town had the largest number of green-space patches, with a total of 234; Boai Subdistrict and Haifu Subdistrict had the fewest patches, each with only four. Some green-space patches were divided by the administrative boundaries of subdistricts and belonged to multiple subdistricts simultaneously, leading to repeated counting of the same patch. Chengxi Town had the highest number of UGSs with cooling effects, reaching 130, whereas Haifu Subdistrict had the fewest, with only one. The CA, defined as the combined extent of UGSs and their cooling ranges, totaled 11,396.08 ha across the study area. Chengxi Town recorded the largest CA of 2051.71 ha, whereas Boai Subdistrict had the smallest, at 77.84 ha. The overall per capita cooling area (CAC) was 55.77 m^2, with Xinbu Subdistrict recording the highest value at 158.90 m^2. Notably, in all subdistricts and townships, the CA exceeded the actual urban green spaces area (UGSA) (Table 2).

Among all urban green spaces, parks with measurable cooling effects were relatively scarce. The park cooling area (PCA) accounted for only 7.88% of the total cooling area and covered merely 5.19% of the study area. And only a small number of subdistricts can enjoy cooling services from parks. However, when all urban green spaces were included, the coverage of cooling services increased significantly to 73.05%. This indicates that non-park urban green spaces play an indispensable role in urban cooling-service provision and that relying solely on park green spaces is insufficient (Table 2).

Table 1. Statistics of cooling effect of green spaces based on subdistrict (township).

Subdistrict (Township)	CI			CD		
	Min	Max	Mean	Min	Max	Mean
Bailong	0.18	2.85	1.24	42.10	520.40	226.80
Baisha	0.09	4.47	1.84	62.90	544.00	278.29
Binhai	0.61	3.30	1.93	28.60	496.40	201.21
Binjiang	0.25	3.54	1.54	52.00	479.30	266.73
Boai	2.21	2.39	2.30	195.20	474.90	335.05
Chengxi	0.16	6.27	2.11	17.80	545.20	242.50
Datong	0.20	2.87	1.56	31.30	465.80	226.98
Fengxiang	0.10	3.86	1.30	37.30	540.60	202.24
Fucheng	0.22	2.24	1.02	90.70	461.60	262.53
Guoxing	0.06	3.85	1.48	45.80	501.80	237.79
Haidian	0.39	4.07	2.37	33.60	540.50	195.91
Haifu	0.53	0.53	0.53	208.80	208.80	208.80
Haiken	0.31	4.80	2.34	74.60	441.90	233.64
Haixiu	0.15	5.95	2.10	22.20	540.50	228.81
Haixiu town	0.20	6.51	2.19	17.80	543.00	225.63
Hepingnan	0.22	3.86	1.70	131.90	509.40	287.67
Jinmao	0.20	5.62	1.79	23.90	489.00	222.69
Jinyu	0.49	4.82	2.45	101.00	463.70	244.80
Lantian	0.43	3.84	1.85	141.80	530.20	350.06
Renminlu	0.22	9.11	2.19	20.00	488.90	206.30
Xinbu	0.12	4.47	1.70	57.10	544.00	195.83
Xiuying	0.35	4.78	2.10	66.70	536.40	223.37
Zhongshan	0.49	3.82	2.25	162.40	474.90	318.85

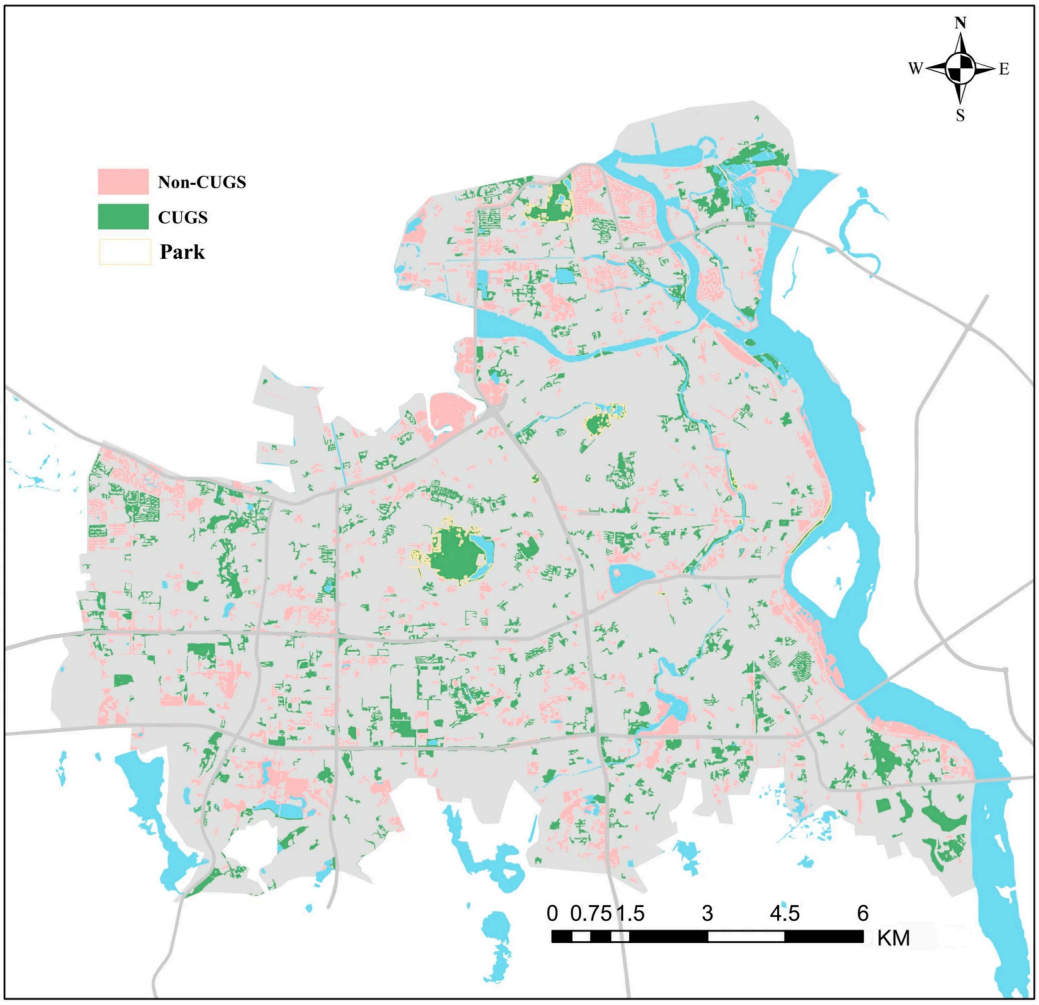


Figure 3. Distribution of cooling UGSs and non-cooling UGSs.

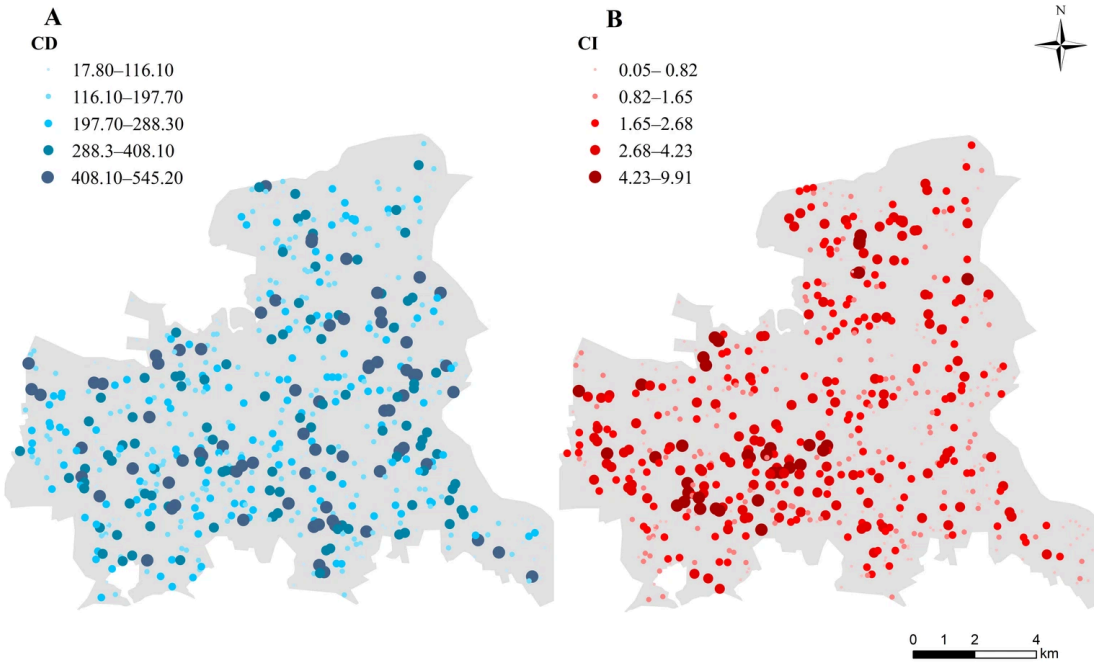


Figure 4. The cooling effect of UGSs in the study area. (**A**) for CD and (**B**) for CI.

https://doi.org/10.3390/land15122270

Table 2. CUGS and CA statistics for subdistrict (township).

Subdistrict (Township)	UGS Count	CUGS Count	UGSA/ha	CA/ha	CAC/m^2	PCA/ha
Bailong	26	14	17.33	293.38	28.00	41.62
Baisha	28	13	20.33	314.38	69.97	0
Binhai	32	18	26.13	272.16	45.47	0
Binjiang	53	27	80.15	513.19	49.05	2.43
Boai	4	2	0.39	77.84	18.59	43.67
Chengxi	234	130	224.22	2051.71	97.35	0
Datong	15	14	17.67	180.89	26.54	91.72
Fengxiang	126	68	165.56	1168.07	60.25	0
Fucheng	27	12	10.94	248.42	20.24	13.16
Guoxing	56	30	51.62	461.08	76.78	111.28
Haidian	53	21	48.58	435.06	42.57	34.75
Haifu	4	1	15.45	144.17	18.24	50.48
Haiken	59	30	126.07	544.57	28.42	238.22
Haixiu	69	32	93.52	598.04	73.52	87.8
Haixiu Town	134	70	100.94	1085.93	136.51	0
Hepingnan	11	6	11.93	110.18	38.48	1.10
Jinmao	67	31	32.09	411.20	50.69	0
Jinyu	32	17	29.41	367.47	50.81	18.21
Lantian	33	14	15.37	277.22	60.05	49.73
Renminlu	85	41	95.38	587.33	50.09	49.76
Xinbu	52	20	78.22	466.95	158.90	0
Xiuying	74	37	68.10	699.10	64.24	0
Zhongshan	6	6	19.31	87.74	34.40	63.82

3.2. Spatial Pattern of Cooling Services Supply and Demand Index

Figure 5 shows the spatial distribution of CSI and CDI. There were pronounced spatial disparities in the supply and demand of cooling services provided by UGSs, with supply and demand showing contrasting spatial distributions. Overall, cooling services supply was primarily distributed around UGSs, with higher supply levels observed in the southwestern part of the study area. High-value areas of the CSI were mainly located in the western, southern, and northeastern parts of the central urban area, particularly near large parks, urban peripheries, UGSs along the Meishe River, and industrial zones. In contrast, low-value areas were concentrated in parts of the northern and eastern regions, as well as along rivers and coastal zones, which were predominantly characterized by dense buildings and high population concentrations in older urban areas (Figure 5A).

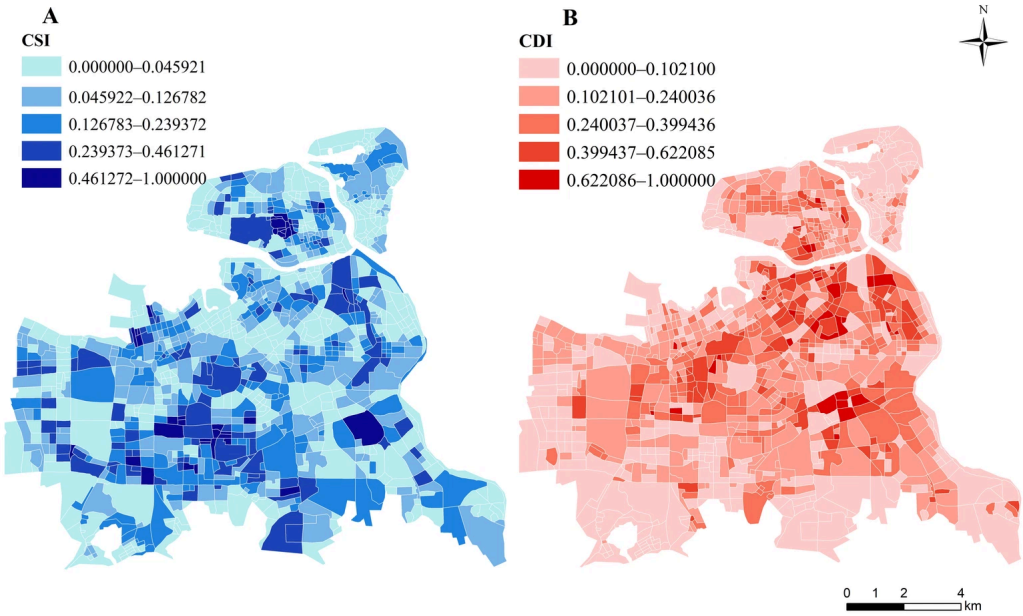


Figure 5. Spatial distribution of Cooling Services Supply and Demand Indices. (**A**) for CSI and (**B**) for CDI.

In terms of demand (CDI), a clear core-periphery pattern was observed, with higher demand in central areas and lower demand toward the outskirts. High-demand areas were mainly located east of the geometric center of the central urban area. Medium-demand areas were the most widespread and were generally distributed around high-demand zones. Low-demand areas were primarily found in the northern coastal zone, the western and southern fringes of the central urban area, and along sections of the Nandu River. Areas with higher demand were typically associated with higher building and population densities (Figure 5B).

The average CSI and CDI across the study area were 0.11 and 0.25, respectively. At the subdistrict (township) level, Hepingnan Subdistrict had the highest average CSI of 0.29, whereas Haifu Subdistrict had the lowest at 0.04 and simultaneously exhibited the highest CDI of 0.53. In contrast, Xinbu Subdistrict recorded the lowest CDI of 0.06 (Figure 6). In the study area, the average demand value of most subdistricts was far higher than the average supply value; only three subdistricts showed a higher supply value than the demand value. Subdistricts (townships) in the old urban area presented high demand accompanied by low supply, while those in the new urban area or suburbs had relatively abundant supply and low demand.

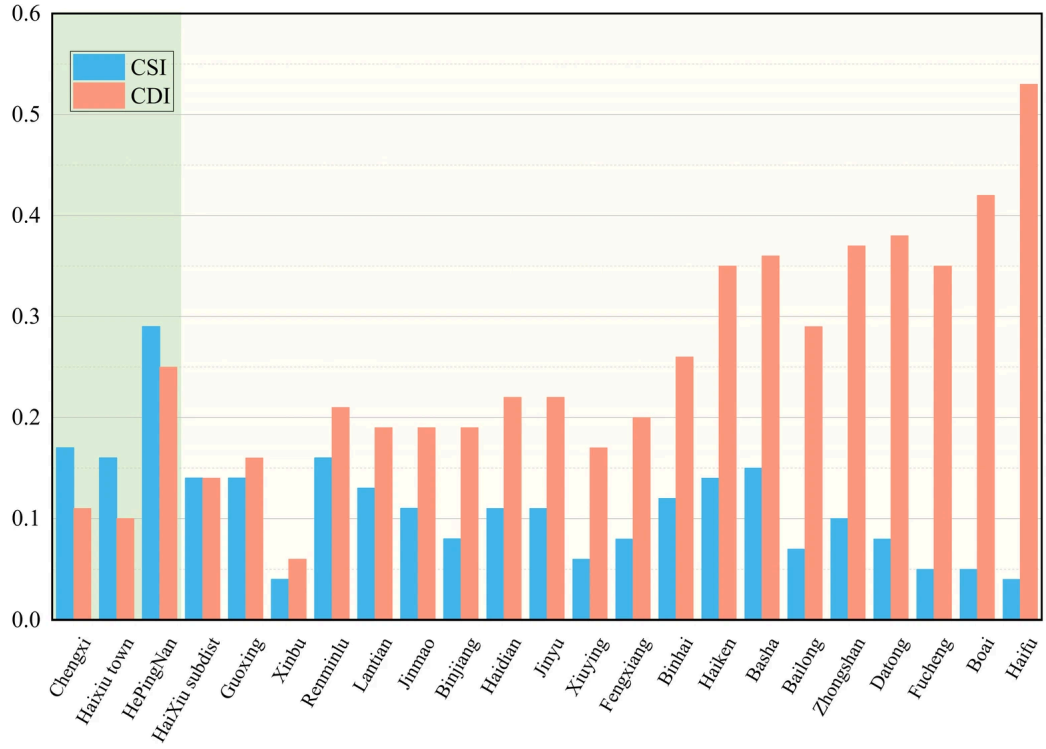


Figure 6. Average CSI and CDI for subdistrict (township).

3.3. Cooling Services Matching and Coordination Characteristics

3.3.1. Types of Supply–Demand Relationship

Based on the supply–demand ratio of cooling services, the study area was predominantly characterized by imbalanced types, whereas balanced types were scarce and appeared only as isolated patches. Overall, the level of supply–demand matching remained relatively low (Figure 7A). The central part of the study area was mainly dominated by deficit and mid-deficit types, interspersed with zero-supply areas where cooling supply failed to meet demand, resulting in pronounced thermal stress. In contrast, the southern suburban area was largely characterized by surplus and mid-surplus types, where cooling resources were relatively abundant and thermal pressure was comparatively low.

The deficit type constituted the largest proportion, accounting for 31.58% of all blocks and encompassing 49.56% of the total population. These blocks were primarily located in densely populated old urban areas. The surplus type represented 13.52% of blocks but served only 5.53% of the population, and was mainly distributed in peripheral areas and the southwestern industrial zone, where cooling supply substantially exceeds demand (Figure 7A).

Zero-supply areas accounted for 21.60% of all blocks and accommodated 18.77% of the population. These areas fell outside the cooling influence range of any UGS, forming distinct blind spots in cooling services provision. In addition, zero-demand blocks had no residents and therefore contained no resident population. In contrast, supply–demand balanced areas were limited, accounting for only 7.15% of the population and exhibiting a fragmented spatial pattern, indicating that well-matched cooling services provision remained scarce (Table 3).

In summary, areas with insufficient supply and zero-supply areas collectively accounted for 63.52% of all blocks yet were home to 79.63% of the total population. This means that the vast majority of residents cannot access adequate cooling services. Such supply–demand mismatch increases heat-related environmental risks in these areas (

Table 3).

At the subdistrict (township) scale, supply–demand imbalance was widespread. Deficit and mid-deficit types dominated, with insufficient cooling supply affecting 15 subdistricts and 61.02% of the population, mainly across central and northern subdistricts (townships). Five subdistricts, namely Hepingnan, Renminlu, Guoxing, Fengxiang, and Haixiu, achieved a balanced supply–demand relationship, accounting for 25.18% of the total area and serving 23.42% of the population. Three subdistricts (townships), namely Chengxi Town, Haixiu Town, and Xinbu Subdistrict, were classified as mid-surplus, accounting for 32.72% of the total area and 15.56% of the resident population (Figure 7B; Table 3).

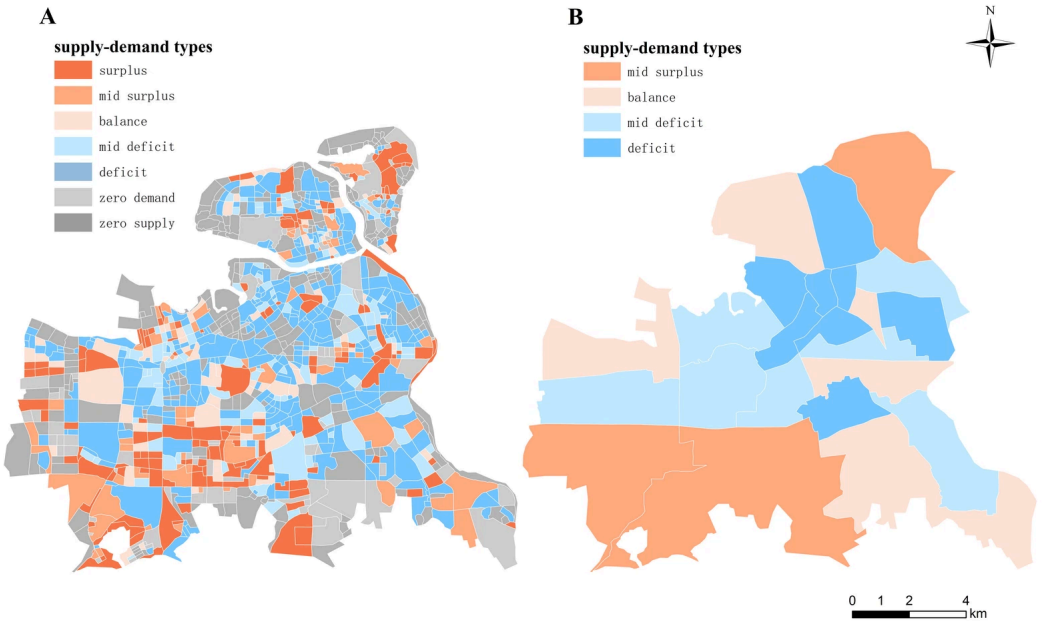


Figure 7. Spatial distribution of supply–demand relationship types. (**A**) at the block scale, (**B**) at the subdistrict (township) scale.

Table 3. Proportions of cooling services supply–demand relationship types.

Supply–Demand Types	Block		Subdistrict	
	Count Ratio (%)	Pop Ratio (%)	Count Ratio (%)	Pop Ratio (%)
surplus	13.52	5.53	0	0
mid-surplus	6.99	7.69	13.04	15.56
balance	6.44	7.15	21.74	23.42
mid-deficit	10.34	11.3	30.43	31.62
deficit	31.58	49.56	34.79	29.4
zero supply	21.6	18.77	0	0
zero demand	9.53	0	0	0

3.3.2. Coupling Coordination Degree (CCD) Analysis

The CCD model was employed to quantify the coordination between the supply and demand of cooling services provided by urban green spaces. The coordination levels were classified into seven stages using the natural breaks (Jenks) method, ranked from high to low: excellent coordination, good coordination, intermediate coordination, initial coordination, barely coordinated, near-disorder, and disorder (Table 4). The results

showed that only 8.44% of the blocks fell into the good or excellent coordination stages, while the remaining 91.56% were below these levels; these blocks accommodated 86.81% of the total population, indicating substantial room for improving supply–demand coordination (Figure 8A; Table 5).

The number of blocks in the excellent coordination stage was extremely small, accounting for only 1.36% of all blocks and 3.65% of the total population. These blocks were sporadically distributed in the central-eastern part of the study area. The intermediate and initial coordination stages together formed a relatively continuous belt across the central part of the study area, occupying 26.68% of the blocks and 36.85% of the population. In contrast, blocks with low coordination levels, including near-disorder and disorder, were mainly distributed in the southwestern, eastern, and northeastern regions, encompassing 17.60% of the population (Figure 8A; Table 5).

At the subdistrict (township) scale, highly coordinated subdistricts cluster in the central-southern core and coastal zone, while low-coordination ones lie in the old urban districts and the northeastern corner; the west is largely initial or barely, and the southeast are dominated by intermediate coordination. The disorder stage occurs only in Xinbu Subdistrict, which holds 1.43% of the population. The two near-disorder subdistricts, Fucheng and Haifu, occupy 4.33% of the area and hold 9.82% of the population. The five good and excellent subdistricts cluster in the central-southern core, accounting for 17.67% of the population and 10.74% of the area.

Table 4. Grading criteria for CCD.

No.	Level	Range	
		Block	Subdistrict
1	disorder	[0.009327, 0.150304]	[0.214005, 0.215002]
2	near-disorder	[0.150304, 0.249996]	[0.215002, 0.301591]
3	barely coordinated	[0.249996, 0.331883]	[0.301591, 0.339874]
4	initial coordination	[0.331883, 0.403410]	[0.339874, 0.356025]
5	intermediate coordination	[0.403410, 0.482283]	[0.356025, 0.403733]
6	good coordination	[0.482283, 0.594990]	[0.403733, 0.470079]
7	excellent coordination	[0.594990, 0.866995]	[0.470079, 0.528993]

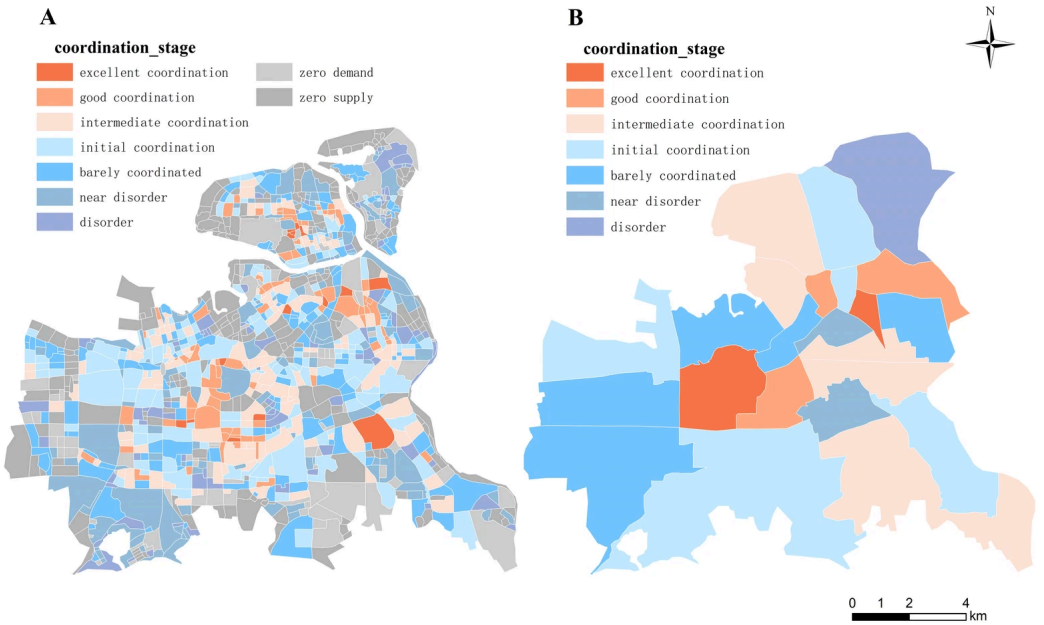


Figure 8. Spatial distribution of CCD. (**A**) At the block scale, (**B**) at the subdistrict (township) scale.

Table 5. Proportions statistics of CCD.

Coordination Stage	Block		Subdistrict	
	Count Ratio (%)	Pop Ratio (%)	Count Ratio (%)	Pop Ratio (%)
disorder	7.26	4.65	4.35	1.43
near-disorder	12.7	12.95	8.7	9.82
barely coordinated	13.79	13.59	21.73	21.53
initial coordination	13.61	20.81	21.74	26.32
intermediate coordination	13.07	16.04	21.74	23.23
good coordination	7.08	9.54	13.04	6.95
excellent coordination	1.36	3.65	8.7	10.72
zero supply	21.6	18.77	0	0
zero demand	9.53	0	0	0

3.4. Composite Classification and Priority Management Areas

Based on the supply–demand matching status and CCD of cooling services provided by UGSs, spatial mismatches and low-coordination areas were overlaid to identify composite types and delineate priority areas for improvement. The results (Figure 9A) indicate that among the 1102 blocks in the central urban area of Haikou, 558 anomalous blocks were identified, accounting for 50.64% of the total. These anomalous areas were primarily distributed in the central old urban area and the peripheral suburban zones, exhibiting a scattered pattern in the urban core and a more contiguous distribution in suburban areas. In terms of type composition, deficit-disorder and deficit-near-disorder blocks accounted for 47 and 97 blocks, respectively, while surplus-disorder and surplus-near-disorder blocks accounted for 33 and 38 blocks. Zero-demand and zero-supply

blocks numbered 105 and 238, respectively (Figure 9A).

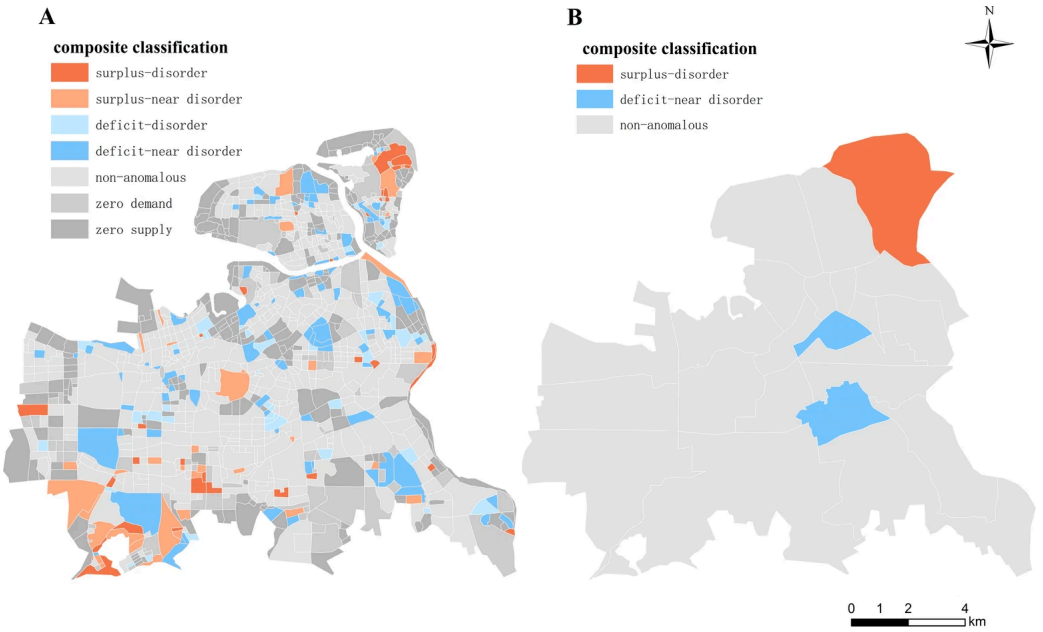


Figure 9. Spatial distribution of composite Classification based on supply–demand coupling coordination degree. (**A**) at the block scale, (**B**) at the subdistrict (township) scale.

Spatially, non-anomalous blocks form the overall background, while anomalous blocks are scattered rather than clustered into continuous large patches. Surplus-disorder areas are mainly distributed in the southwestern and northeastern suburbs, where cooling supply is abundant, but demand is low, resulting in a severe supply–demand imbalance and poor coordination. These areas are characterized by extensive UGS cover, low population density, and relatively low LST, which together lead to limited cooling demand. In contrast, deficit-disorder areas form a belt along the eastern part and are scattered across the urban core, showing insufficient cooling resources, high population density, high heat exposure, and strong cooling demand. Zero-supply and zero-demand blocks are mostly distributed in the western and northwestern parts and the urban fringe, which constitute key areas for thermal environment management (Figure 9A).

From a population perspective, the priority areas involve 746,000 residents, accounting for 36.31% of the total population. Among the residents in these priority areas, 51.71% are located in zero-supply areas, indicating that the most severe supply–demand conflicts are concentrated in densely populated areas. Deficit-disorder and deficit-near-disorder areas account for 45.80% of the population in the priority areas and belong to secondary priority. In contrast, surplus-near-disorder, surplus-disorder, and zero-demand areas together account for only 2.50% of this population, suggesting that, despite the resource surplus, their direct impact is limited (Table 6).

At the subdistrict scale, Haifu and Fucheng Subdistricts are classified as deficit-near-disorder, occupying 4.33% of the total area and 9.82% of the population; these areas are mainly located in the core of the old urban district. Only Xinbu Subdistrict is classified as surplus-disorder, occupying 5.47% of the total area and 1.43% of the population (Table 6).

Overall, zero-supply areas are the highest-priority intervention targets, as they exhibit the most severe supply–demand imbalance. Deficit-disorder and deficit-near-disorder areas belong to the second priority, whereas surplus-related types have limited impact on the population despite their abundant resources and are therefore assigned a

lower priority (Figure 9 and Table 6).

Table 6. Proportions of supply–demand coupling coordination types.

Priorities	Composite Classification	Block		Subdistricts	
		Count Ratio (%)	Pop Ratio (%)	Count Ratio (%)	Pop Ratio (%)
I	zero supply	21.6	18.77	0	0
II	deficit-disorder	4.26	4.58	0	0
III	deficit-near-disorder	8.8	12.05	8.7	9.82
IV	surplus-disorder	2.99	0.07	4.35	1.43
	surplus-near-disorder	3.45	0.83	0	0
	non-anomalous	49.37	63.7	86.95	88.75
	zero demand	9.53	0	0	0

4. Discussion and Suggestions

4.1. Discussion

In this study, UGSs without a detectable cooling effect were predominantly located in coastal zones, along the Nandu River, and in the vicinity of large water bodies. The CD of UGSs ranged from 17.8 m to 545.2 m, with a mean value of 231.98 m, while CI varied between 0.06 °C and 9.11 °C, averaging 1.92 °C. Notably, UGSs adjacent to large water bodies exhibited no measurable cooling effect. This finding is consistent with previous studies reporting that water bodies generally exert stronger cooling effects than vegetated areas, characterized by greater CI and a broader cooling extent, which may mask or override the cooling effect of surrounding UGSs [50,51].

A pronounced spatial mismatch between cooling services supply and demand was observed. Cooling supply was primarily concentrated in peripheral suburban areas and certain industrial zones, whereas cooling demand was largely clustered in old urban districts. On the one hand, suburban areas are characterized by extensive UGS coverage and low building density, which facilitate heat exchange between UGSs and their surrounding environment, thereby forming stable cool islands and enhancing cooling supply capacity [52,53]. On the other hand, industrial zones are dominated by high proportions of impervious surfaces and substantial anthropogenic heat emissions, resulting in elevated LST. Under these conditions, stronger thermal gradients between UGSs and their surroundings may enhance the observable cooling effect of individual green patches [54]. In contrast, high-demand areas are characterized by limited UGS availability, reduced cooling efficiency, and persistently high LST. These areas are typically associated with long-term urban development, fragmented planning structures, and densely packed and irregular building configurations, which restrict the spatial diffusion of cooling effects and contribute to both high population density and elevated cooling demand.

This study assessed the cooling area of all UGSs, including both PUGSs and NPUGSs. Ke et al. suggested that incorporating NPUGSs into analyses can significantly improve the equity of UGS accessibility [55]. In this study, when other types of UGSs were incorporated, the coverage of cooling services increased significantly from 5.19% to 73.05%, indicating a marked improvement in cooling-service coverage. This result indi-

cates that NPUGSs play a critical complementary role in mitigating urban heat exposure and expanding the spatial extent of cooling services, which may otherwise be underestimated when only PUGSs are considered.

The study area was predominantly characterized by imbalanced supply–demand types, while balanced types were rare and appeared only as isolated patches, indicating weak overall alignment between cooling supply and demand. At the subdistrict (township) scale, deficit and mid-deficit were the dominant supply–demand matching types, affecting 61.02% of the population. Moreover, the CCD reflects the extent to which the supply and demand systems interact in a mutually promoting or constraining manner. Overall, 91.56% of the blocks had not reached a relatively high level of coordination, encompassing 86.81% of the total population in the study area. Several subdistricts (townships), particularly in the old urban area, were identified as being in a state of disorder or near-disorder. This pattern indicates that cooling services provision is not only insufficient in magnitude but also spatially mismatched with areas of high population exposure, reflecting both structural deficits in UGS supply and systemic inefficiencies in spatial allocation.

The comparison reveals no consistent spatial correspondence between supply–demand type and coupling coordination stage. In the central part of the study area, deficit and mid-deficit types prevail, yet most blocks fall into the Initial or Intermediate coordination stages; mid-deficit blocks are generally at a moderate coordination level, whereas some deficit blocks remain in the near-disorder or barely coordinated stage. In the southwestern part, surplus blocks dominate but generally show low coordination, falling mainly into low-coordination stages such as near-disorder, disorder, and barely coordinated. This indicates that surplus does not equal coordination, and deficit does not necessarily imply disorder. This may be because the central area consists largely of planned residential neighborhoods with an existing green-space base and a lower population density than the old urban district, so cooling demand pressure is relatively modest and supply–demand coordination remains moderate. In the southwestern suburbs, green spaces are relatively abundant, but the population is sparse, and cooling demand is weak, producing a large supply–demand gap and a low coupling degree. These findings highlight the need for targeted policy interventions to improve the alignment between cooling supply and demand.

The CCD model applied in this study has been widely used in assessing the supply–demand relationships of UGS ecosystem services. Consistent with previous studies, Gao et al. reported generally low coupling coordination of cooling services in Urumqi, while Shen et al. similarly found suboptimal coordination between cooling supply and demand in the Fujian Delta urban agglomeration [56,57]. These consistent findings across different urban contexts further confirm that insufficient coordination between cooling supply and demand is a widespread issue in rapidly urbanizing regions.

4.2. Urban Planning and Policy Recommendations

In response to the problems of supply–demand imbalance of cooling services in the central urban area of Haikou, the following strategic recommendations are proposed.

For zero-supply areas, which lack UGS cooling services and have the most urgent cooling demand, green coverage should be expanded through pocket parks, street greenery, shared affiliated green spaces, and rooftop and vertical greening; existing scattered patches should be upgraded with multilayered communities, while cool pavements and shade facilities serve as supplementary measures where land is scarce [4,58].

For blocks and subdistricts (townships) of the deficit-disorder type, the following measures are suggested. In coastal blocks, the construction of shade-providing UGSs

should be increased. By planting trees with large canopy coverage, physical shading can reduce LST. Low-canopy shrubs or lawns should be arranged downwind of the prevailing wind direction to create ventilation corridors that facilitate the penetration of sea breezes and lower ambient temperatures [58,59]. In areas with dense built-up structures and limited UGS resources, existing UGS patches should be upgraded, and the spatial pattern and vegetation composition of UGSs should be re-optimized to improve cooling efficiency. In addition, measures such as roof greening, vertical greening, roadside greening, pocket greening, and three-dimensional greening should be adopted to enhance the supply of UGS cooling resources and reduce supply–demand imbalances [60,61].

For blocks and subdistricts (townships) of the surplus-disorder; surplus-near-disorder types, and zero demand, which are mostly located in urban suburbs with abundant UGS cooling resources but sparse populations, potential future population influx should be anticipated. High-density development should be restricted, and ecological red lines should be established to maintain the existing scale of green-space patches. At the same time, spatial structures should be optimized to preserve the connectivity of the cooling network, and ecological corridors should be constructed to enhance the cooling efficiency of large UGS patches [62].

For non-priority areas, development intensity should be controlled to avoid exacerbating the thermal environment. The spatial layout of UGSs should be optimized to strengthen the cooling effect of existing UGSs. Moreover, the dynamic monitoring of changes in UGSs, LST, and population in these areas is necessary to identify risks of supply–demand imbalance in advance [63,64].

4.3. Limitations and Future Research

Nevertheless, this study involved certain limitations. It relied on Landsat 8 data from a single summer season, without accounting for the long-term evolution of the supply–demand balance of UGS cooling services or the dynamic differences in thermal environments between seasons and between day and night. Future research should incorporate multi-temporal data to investigate the spatiotemporal evolution of cooling-service supply and demand. In addition, constrained by the spatial resolution of the data, small green patches were not included in this study, although such small green spaces may be of considerable importance. Moreover, the equity analysis in this study did not account for differences among social groups, such as vulnerable populations. Future studies could integrate social attributes, including age and income, to provide a more comprehensive assessment of the social equity of cooling resource allocation. Finally, this study characterized the spatial matching pattern of cooling-service supply and demand but did not identify the factors influencing this matching. Future work should combine multi-source environmental and socioeconomic data to further investigate the determinants of the supply–demand matching of UGS cooling services.

5. Conclusions

This study assessed the supply–demand matching and coupling coordination of UGS cooling services in central Haikou using the supply–demand ratio and CCD model and identified composite priority types across 1102 blocks and 23 subdistricts (townships). The main conclusions are as follows:

Only 54.73% of UGS patches showed a measurable cooling effect, with a mean CD of 231.98 m and mean CI of 1.92 °C. Cooling supply was concentrated in suburban peripheries and industrial zones, while demand clustered in dense old urban areas; imbalanced types dominated, with deficit, mid-deficit, and zero-supply blocks covering

79.63% of the population, and 91.56% of blocks and 86.81% of the population remained below good or excellent coordination. In total, 50.64% of blocks were anomalous and covered 36.31% of the population, with zero-supply, deficit-disorder, and deficit-near-disorder accounting for 97.51% of the priority population. These results provide a spatial basis for targeting cooling deficits and guiding equitable urban greening in tropical cities.

In summary, this study developed an analytical framework that integrates the supply–demand ratio and the coupling coordination degree (CCD) model to evaluate the supply–demand matching and coordination of cooling services provided by urban green spaces. The framework provides a methodological approach for assessing cooling-service equity and urban thermal environment management. Unlike previous assessments that focus on large urban parks and rely on descriptive surplus/deficit mapping, this framework incorporates park green spaces and non-park urban green spaces and jointly characterizes the quantitative matching and systemic interaction between supply and demand, thereby advancing the evaluation of cooling services. By conducting the analysis at both the block and subdistrict scales, the study reveals spatial heterogeneity in cooling-service supply–demand relationships across spatial levels and supports more targeted and refined decision-making for thermal environment governance. The findings can assist urban planners and policymakers in optimizing the allocation of cooling services, improving the efficiency of urban green spaces planning and management, and ultimately promoting sustainable urban development.

Author Contributions: Conceptualization, Y.D.; methodology, Y.D.; software, Y.H.; formal analysis, Y.H.; data curation, Z.R. and Y.Z.; writing—original draft preparation, Y.H.; writing—review and editing, Y.H.; visualization, Z.R. and Y.Z.; supervision, Y.D. All authors have read and agreed to the published version of the manuscript.

Funding: This research was supported by the National Key R & D Program of China (grant number: 2023YFF1304600), the National Natural Science Foundation of China (grant number: 42571121) and the Hainan Provincial Natural Science Foundation of China (grant number: 724MS059).

Data Availability Statement: The data that support the findings of this study are available from the corresponding author upon reasonable request. The data are not publicly available due to privacy and research project restrictions.

Conflicts of Interest: The authors declare no conflicts of interest.

References

1. Liu, Y.; An, Z.; Ming, Y. Simulating influences of land use/land cover composition and configuration on urban heat island using machine learning. *Sustain. Cities Soc.* **2024**, *108*, 105482. [Google Scholar] [CrossRef]
2. Aghazadeh, F.; Samadi, M.; Cheval, S.; Moshiri, S. Impacts of land use, vegetation, and air pollution on surface urban heat island spatiotemporal dynamics: Tehran as a case study. *Int. J. Environ. Sci. Technol.* **2025**, *22*, 14607–14633. [Google Scholar] [CrossRef]
3. Ho, J.Y.; Shi, Y.; Lau, K.K.; Ng, E.Y.; Ren, C.; Goggins, W.B. Urban heat island effect-related mortality under extreme heat and non-extreme heat scenarios: A 2010–2019 case study in Hong Kong. *Sci. Total Environ.* **2023**, *858*, 159791. [Google Scholar] [CrossRef] [PubMed]
4. Zhang, Z.; Lv, Y.; Pan, H. Cooling and humidifying effect of plant communities in subtropical urban parks. *Urban For. Urban Green.* **2013**, *12*, 323–329. [Google Scholar] [CrossRef]
5. Wu, Q.; Huang, Y.; Irga, P.; Kumar, P.; Li, W.; Wei, W.; Shon, H.K.; Lei, C.; Zhou, J.L. Synergistic control of urban heat island and urban pollution island effects using green infrastructure. *J. Environ. Manag.* **2024**, *370*, 122985. [Google Scholar] [CrossRef] [PubMed]

6. Rahman, M.A.; Stratopoulos, L.M.; Moser-Reischl, A.; Zölch, T.; Häberle, K.-H.; Rötzer, T.; Pretzsch, H.; Pauleit, S. Traits of trees for cooling urban heat islands: A meta-analysis. *Build. Environ.* **2020**, *170*, 106606. [Google Scholar] [CrossRef]
7. Zeng, P.; Liu, Y.; Tian, T.; Che, Y.; Helbich, M. Geographic inequalities in park visits to mitigate thermal discomfort: A novel approach based on thermal differences and cellular population data. *Urban For. Urban Green.* **2024**, *98*, 128419. [Google Scholar] [CrossRef]
8. Zhang, M.; Wang, J.; Zhang, F. The influence of spatial heterogeneity of urban green space on surface temperature. *Forests* **2024**, *15*, 878. [Google Scholar] [CrossRef]
9. Wu, Z.; Zhang, Y. Spatial variation of urban thermal environment and its relation to green space patterns: Implication to sustainable landscape planning. *Sustainability* **2018**, *10*, 2249. [Google Scholar] [CrossRef]
10. Zhang, Q.; Zhou, D.; Xu, D.; Rogora, A. Correlation between cooling effect of green space and surrounding urban spatial form: Evidence from 36 urban green spaces. *Build. Environ.* **2022**, *222*, 109375. [Google Scholar] [CrossRef]
11. Lu, Y.; Wu, J.; Liu, M. Decoding the cooling potential of urban green spaces: A cross-city investigation of driving factors in 311 Chinese cities under varying climate zones. *Sustain. Cities Soc.* **2025**, *126*, 106410. [Google Scholar] [CrossRef]
12. Koc, C.B.; Osmond, P.; Peters, A. Evaluating the cooling effects of green infrastructure: A systematic review of methods, indicators and data sources. *Sol. Energy* **2018**, *166*, 486–508. [Google Scholar] [CrossRef]
13. Yu, J.; Zhao, Q.; Gao, L.; Meng, Q.; Lei, X. Surface urban heat islands in coastal and inland cities: A global analysis of drivers and of spatial heterogeneity. *Build. Environ.* **2026**, *301*, 114751. [Google Scholar] [CrossRef]
14. Best, L.; Schwarz, N.; Obergh, D.; Teuling, A.; Van Kanten, R.; Willemen, L. Urban green spaces and variation in cooling in the humid tropics: The case of Paramaribo. *Urban For. Urban Green.* **2023**, *89*, 128111. [Google Scholar] [CrossRef]
15. He, J.; Wang, W.; Teng, Z.; Guo, Z. Cooling accessibility of urban parks: Unraveling spatial disparity and nonlinear drivers using an improved polynomial-2SFCA model and explainable machine learning. *Sustain. Cities Soc.* **2026**, *147*, 107529. [Google Scholar] [CrossRef]
16. Zhou, Y.; Zhao, H.; Luo, Y.; Yi, X.; Lun, F. Exploring the inequality in urban parks' distribution and their cooling effects from the perspective of urbanization. *Landsc. Urban Plan.* **2025**, *260*, 105390. [Google Scholar] [CrossRef]
17. Liu, Z.; Han, Y.; Zheng, H.; Wu, W.; Chen, M.; Peng, D. Equity of cooling services of urban green spaces from the perspective of community life circles: Integrating cooling effects, service quality, and resident preferences. *Trees For. People* **2026**, *23*, 101132. [Google Scholar] [CrossRef]
18. Yu, S.; Zeng, P.; Xie, X.; Chen, D. Equitable evaluation of supply-demand and layout optimization of urban park green space in high-density linear large city. *PLoS ONE* **2024**, *19*, e0310015. [Google Scholar] [CrossRef] [PubMed]
19. Yang, Y.; Wu, Y.; Jiao, H. Assessing urban park equity in China through supply and demand balance: A case study of Wuhan city, China. *Sustainability* **2025**, *17*, 2255. [Google Scholar] [CrossRef]
20. Liu, H.; Remme, R.P.; Hamel, P.; Nong, H.; Ren, H. Supply and demand assessment of urban recreation service and its implication for greenspace planning-A case study on Guangzhou. *Landsc. Urban Plan.* **2020**, *203*, 103898. [Google Scholar] [CrossRef]
21. Fei, W.; Lu, D.; Li, Z. Research on the layout of urban disaster-prevention and risk-avoidance green space under the improvement of supply and demand match: The case study of the main urban area of Nanjing, China. *Ecol. Indic.* **2023**, *154*, 110657. [Google Scholar] [CrossRef]
22. Zhang, Q.; Jiang, R.; Jiang, X.; Li, Y.; Cong, X.; Xiong, X. Supply–Demand Spatial Patterns of Cultural Services in Urban Green Spaces: A Case Study of Nanjing, China. *Land* **2025**, *14*, 1044. [Google Scholar] [CrossRef]
23. Wang, Y.; Ouyang, W.; Zhang, J. Matching supply and demand of cooling service provided by urban green and blue space. *Urban For. Urban Green.* **2024**, *96*, 128338. [Google Scholar] [CrossRef]
24. Xia, T.; Zhang, L.; Zou, Y. Mismatch Between Heat Exposure Risk and Blue-Green Exposure in Wuhan: A Coupled Spatial Analysis. *Sustainability* **2025**, *17*, 8440. [Google Scholar] [CrossRef]
25. Luo, C.; Li, X. Assessment of ecosystem service supply, demand, and balance of urban green spaces in a typical mountainous city: A case study on Chongqing, China. *Int. J. Environ. Res. Public Health* **2021**, *18*, 11002. [Google Scholar] [CrossRef] [PubMed]
26. Dong, Y.; Chen, X.; Lv, D.; Wang, Q. Evaluation of urban green space supply and demand based on mobile signal data: Taking the central area of Shenyang city as an example. *Land* **2023**, *12*, 1742. [Google Scholar] [CrossRef]
27. Chen, H.; Liu, Z.; Hu, L.; Li, Z.; Chen, J. Integrating blue and green spaces: Multi–dimensional equity evaluation of urban green–blue spaces distribution based on coupling theory in Hangzhou. *Local Environ.* **2026**, 1–27. [Google Scholar] [CrossRef]

28. Wang, L.; Yuan, M.; Li, H.; Chen, X. Exploring the coupling coordination of urban ecological resilience and new-type urbanization: The case of China's Chengdu–Chongqing Economic Circle. *Environ. Technol. Innov.* **2023**, *32*, 103372. [Google Scholar] [CrossRef]
29. Huang, G.; Liu, S.; Cai, B.; Wang, B. The coupling coordination of social and economic upgrading in China: Evolution, regional disparities and influencing factors. *J. Geogr. Sci.* **2024**, *34*, 835–854. [Google Scholar] [CrossRef]
30. Wang, J.; Hou, H.; Zhang, S.; Zhang, S.; Ji, H.; Chen, Z. Coupling coordination between ecosystem services and sustainable development goals from a county-level perspective in Jiangsu Province, China. *Land* **2025**, *14*, 1627. [Google Scholar] [CrossRef]
31. Moncada-Morales, G.A.; Verichev, K.; López-Guerrero, R.E.; Carpio, M. A Global Review of Vegetation's Interaction Effect on Urban Heat Mitigation Across Different Climates. *Urban Sci.* **2025**, *9*, 361. [Google Scholar] [CrossRef]
32. Ching, G.N.Y.; Yik, S.K.; Heng, S.L.; Ho, B.H.; Crank, P.J.; Mandelmilch, M.; Ho, X.T.; Chow, W.T.L. Park cool island modifications to assess radiative cooling of a tropical urban park. *Sci. Rep.* **2025**, *15*, 15355. [Google Scholar] [CrossRef] [PubMed]
33. Ossola, A.; Jenerette, G.D.; McGrath, A.; Chow, W.; Hughes, L.; Leishman, M.R. Small vegetated patches greatly reduce urban surface temperature during a summer heatwave in Adelaide, Australia. *Landsc. Urban Plan.* **2021**, *209*, 104046. [Google Scholar] [CrossRef]
34. Herreros-Cantis, P.; McPhearson, T. Mapping supply of and demand for ecosystem services to assess environmental justice in New York City. *Ecol. Appl.* **2021**, *31*, e02390. [Google Scholar] [CrossRef] [PubMed]
35. Xu, Z.; Zhao, S. Fine-grained urban blue-green-gray landscape dataset for 36 Chinese cities based on deep learning network. *Sci. Data* **2024**, *11*, 266. [Google Scholar] [CrossRef] [PubMed]
36. Yang, C.; He, X.; Wang, R.; Yan, F.; Yu, L.; Bu, K.; Yang, J.; Chang, L.; Zhang, S. The effect of urban green spaces on the urban thermal environment and its seasonal variations. *Forests* **2017**, *8*, 153. [Google Scholar] [CrossRef]
37. *Standard's GB 50180-2018*; Standard for Urban Residential Area Planning and Design. Ministry of Housing and Urban-Rural Development: Beijing, China, 2018.
38. Zhang, Y.; Zhao, H.; Long, Y. CMAB: A multi-attribute building dataset of China. *Sci. Data* **2025**, *12*, 430. [Google Scholar] [CrossRef] [PubMed]
39. Wang, S.; Tian, Y.; Zhou, Y.; Liu, W.; Lin, C. Fine-scale population estimation by 3D reconstruction of urban residential buildings. *Sensors* **2016**, *16*, 1755. [Google Scholar] [CrossRef] [PubMed]
40. Zhang, J.; Zhang, H.; Qi, R. A study of size threshold for cooling effect in urban parks and their cooling accessibility and equity. *Sci. Rep.* **2024**, *14*, 16176. [Google Scholar] [CrossRef] [PubMed]
41. Peng, J.; Dan, Y.; Qiao, R.; Liu, Y.; Dong, J.; Wu, J. How to quantify the cooling effect of urban parks? Linking maximum and accumulation perspectives. *Remote Sens. Environ.* **2021**, *252*, 112135. [Google Scholar] [CrossRef]
42. Xie, H.; You, M.; Xiao, Y.; Liu, X.; Li, S.; Liu, J.; Guan, C.; Bao, Z.; Gao, X. A supply-demand evaluation framework for uncovering age and gender inequities in urban green space cooling-A case study of Fuzhou. *Urban For. Urban Green.* **2025**, *116*, 129172. [Google Scholar] [CrossRef]
43. Heng, S.L.; Chow, W.T. How 'hot'is too hot? Evaluating acceptable outdoor thermal comfort ranges in an equatorial urban park. *Int. J. Biometeorol.* **2019**, *63*, 801–816. [Google Scholar] [CrossRef] [PubMed]
44. Hu, J.; Lyu, C.; Hou, Y.; Zhu, N.; Liu, K. Research on Summer Indoor Air Conditioning Design Parameters in Haikou City: A Field Study of Indoor Thermal Perception and Comfort. *Sustainability* **2024**, *16*, 3864. [Google Scholar] [CrossRef]
45. Xie, L.; Liu, S.L.; Dai, H.X.; You, M.Z.; Xiao, Y.; Jiang, Y.J.; Liu, X.Z. Assessment of Urban Green Space Cooling Benefits from a Supply–Demand Matching Perspective: A Case Study of Fuzhou City's Main Urban Area. *Acta Ecol. Sin.* **2025**, *45*, 23. (In Chinese) [Google Scholar]
46. Han, J.; Huang, S.; Zhang, S.; Lin, Q.; Wang, X. Assessing Supply and Demand Discrepancies of Urban Green Space in High-Density Built-Up Areas Based on Vitality Impacts: Evidence from Beijing's Central Districts, China. *Sustainability* **2025**, *17*, 4828. [Google Scholar] [CrossRef]
47. Gan, H.; Feng, J.; Zhao, Z.; Ma, L.; Di, S.; Wen, Y. Identifying the Response of Ecological Well–Being to Ecosystem Services of Urban Green Space Using the Coupling Coordination Degree Model: A Case Study of Beijing, China, 2015–2023. *Forests* **2024**, *15*, 1494. [Google Scholar] [CrossRef]
48. Wang, H.; Yang, Y.; Liu, S.; Xue, H.; Xu, T.; He, W.; Gao, X.; Jiang, R. Unveiling the coupling coordination and interaction mechanism between the local heat island effect and urban resilience in China. *Sustainability* **2024**, *16*, 2306. [Google Scholar] [CrossRef]

49. Fang, Y.; Zhao, L. Exploring the supply-demand match and drivers of blue-green spaces cooling in Wuhan Metropolis. *Urban Clim.* **2024**, *58*, 102194. [Google Scholar] [CrossRef]
50. Sun, X.; Tan, X.; Chen, K.; Song, S.; Zhu, X.; Hou, D. Quantifying landscape-metrics impacts on urban green-spaces and water-bodies cooling effect: The study of Nanjing, China. *Urban For. Urban Green.* **2020**, *55*, 126838. [Google Scholar] [CrossRef]
51. Tan, X.; Sun, X.; Huang, C.; Yuan, Y.; Hou, D. Comparison of cooling effect between green space and water body. *Sustain. Cities Soc.* **2021**, *67*, 102711. [Google Scholar] [CrossRef]
52. Aram, F.; García, E.H.; Solgi, E.; Mansournia, S. Urban green space cooling effect in cities. *Heliyon* **2019**, *5*, e01339. [Google Scholar] [CrossRef] [PubMed]
53. Bi, S.; Tian, Z.; Zhang, Y.; Dai, F. The role of urban green space morphology and threshold in cooling efficiency: Evidence from five cities, China. *J. Clean. Prod.* **2025**, *509*, 145580. [Google Scholar] [CrossRef]
54. Wang, Y.; Ren, Y. Cooling efficiency of urban green spaces across functional zones: Mitigating heat island effects through spatial configuration. *Sustainability* **2025**, *17*, 2275. [Google Scholar] [CrossRef]
55. Ke, X.; Huang, D.; Zhou, T.; Men, H. Contribution of non-park green space to the equity of urban green space accessibility. *Ecol. Indic.* **2023**, *146*, 109855. [Google Scholar] [CrossRef]
56. Gao, L.; Kasimu, A.; Zhang, Y. Research on the Supply-Demand Matching of Blue–Green Spaces in Oasis Cities in Arid Regions: A Case Study of the Three-Ring Area in Urumqi. *Urban Sci.* **2025**, *10*, 12. [Google Scholar] [CrossRef]
57. Shen, Z.-J.; Zhang, B.-H.; Xin, R.-H.; Liu, J.-Y. Examining supply and demand of cooling effect of blue and green spaces in mitigating urban heat island effects: A case study of the Fujian Delta urban agglomeration (FDUA), China. *Ecol. Indic.* **2022**, *142*, 109187. [Google Scholar] [CrossRef]
58. Cheela, V.S.; John, M.; Biswas, W.; Sarker, P. Combating urban heat island effect—A review of reflective pavements and tree shading strategies. *Buildings* **2021**, *11*, 93. [Google Scholar] [CrossRef]
59. Zhang, Y.; Li, X.; Liu, S.; Liu, Z.; Li, Y. The Cooling Effects of Greening Strategies Within High-Density Urban Built-Up Areas in Coastal Slope Terrain. *Sustainability* **2025**, *17*, 11054. [Google Scholar] [CrossRef]
60. Liao, J.; Tan, X.; Li, J. Evaluating the vertical cooling performances of urban vegetation scenarios in a residential environment. *J. Build. Eng.* **2021**, *39*, 102313. [Google Scholar] [CrossRef]
61. Dong, Q.; Lu, H.; Luo, X.; He, P.; Li, D.; Wu, L.; Wei, Y.; Chen, X. Evaluation and optimization of green space fairness in urban built-up areas based on an improved supply and demand model: A Case Study of Chengdu, China. *Sustainability* **2023**, *15*, 15014. [Google Scholar] [CrossRef]
62. Luo, J.; Zhu, L.; Fu, H. A new framework for mitigating urban heat island effect from the perspective of network. *Ecol. Indic.* **2025**, *170*, 113059. [Google Scholar] [CrossRef]
63. Wang, Z.; Liu, Y.; Wang, T.; Tang, S.; Wu, X. Supply and demand analysis of urban thermal environments regulation services from an accessibility perspective: A coupled thermal risk and green space cooling assessment model. *Urban Clim.* **2025**, *60*, 102356. [Google Scholar] [CrossRef]
64. Li, X.; Qian, W.; Chen, Y. Identifying and prioritizing key zones for heat mitigation in Nanjing: A cooling demand-supply mismatch perspective. *Urban Clim.* **2026**, *65*, 102791. [Google Scholar] [CrossRef]

Disclaimer/Publisher's Note: The statements, opinions and data contained in all publications are solely those of the individual author(s) and contributor(s) and not of MDPI and/or the editor(s). MDPI and/or the editor(s) disclaim responsibility for any injury to people or property resulting from any ideas, methods, instructions or products referred to in the content.